Analysis of Sound Attenuation Chambers in Duct System by the Finite Element Method

유한요소법에 의한 소음챔버의 감음특성해석

Seok Joo Choi*, Hideki Tachibana**
崔 錫 柱*, 橘 秀 樹**

ABSTRACT

A new theoretical approach is propsed to estimate the transmission loss of the sound attenuation chambers in HVAC duct system using finite element method. The sound transmission loss can be obtaned by separacting the net sound intensity into progressive and reflected intensities. Within the framework of the proposal, numerical analyses and experiments are executed for the models of different shapes at various boundary conditions. It is shown that the theoretical results are consistent with the experimetal ones.

요 약

공조덕트계에 소음챔버를 설치하여 발생되는 음향투과손실을 유한요소법에 의하여 산출하는 방법을 검토하였다. 여기서는 음장내의 네트음향인텐시티를 입사파와 반사파의 인텐시티로 분리하므로서 투과손실의 산출을 가능하게 하였다. 산출방법의 타당성을 검증하기위하여 형상과 내부흡음조건이 다른 소음챔버를 대상으로 수치해석과 모형실험을 실시한 결과, 양자는 잘 일치하였다.

I. Introduction

Sound attenuation chambers are commonly made use of to reduce the noise in HVAC duct system. When a chamber is to be used inside a building, it is important to estimate the sound transmission loss in the design phase of the chamber. Since a general sound attenuation cha mber is complicated in shape and boundary condition, the transmission loss cannot be obtained by a simple theoretical approach. Many numerical analyses, based on the finite element methods have been applied to solve the problems under the assumption that sound transmission loss is the ratio of the sound pressure at the inlet to the pressure at the outlet ducts of a chamber[1-3]. However, most of the real chambers used for halls have three-dimensional sound fields, considering that their associated frequencies and the power of the sound source varies due to the change of the termination impedance. In this case the transmission loss should be considered as the ratio between the incident power and the transmitted power in the chamber.

*Samsung Engineering and Construction Co.Ltd.
**Tokyo University
접수일자 : 1993. 6. 9

In this paper a new theoretical approach will be presented within the framework of finite element analysis for the estimation of the transmission loss in a sound attenuation chamber, independent of dimensions or shapes. Also, a method of estimating the experimental measurements will be discussed. Numerical analyses and scale model experiments are carried out for sound attenuation chambers of different shapes, and the results are compared.

Ⅱ. Numerical Analysis

2.1 Finite Element Formulation of Helmholtz Equation

When a harmonic vibration is assumed in a wave equation, the Helmholtz equation is obtained as follows[4]:

$$\nabla^2 p + \frac{\omega^2}{c_0^2} p = 0 \qquad \text{in } \Omega \tag{1}$$

where ∇^2 is the Laplacian, c_0 is the speed of sound in air(m/sec), p is the complex sound pressure, and Ω is the sound field domain(its boundary $\partial\Omega$ included).

By multiplying Eq.(1) by a weighting fuction Φ followed by the integration over the sound field domain Ω in Fig.1, the Eq.(1) becomes

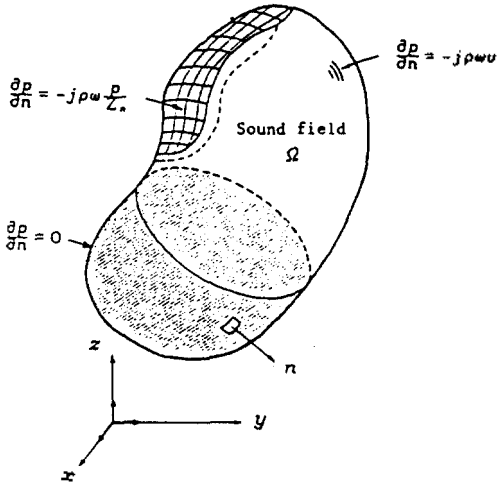

Fig. 1. Boundary conditions of 3-dimensional sound field.

$$\int_\Omega \Phi \cdot \left[\left(\frac{\partial^2 p}{\partial x^2} + \frac{\partial^2 p}{\partial y^2} + \frac{\partial^2 p}{\partial z^2} \right) + \frac{\omega^2}{c_0^2} p \right] dxdydz \tag{2}$$

Based on the Green Theorem, Eq.(2) can be expressed as:

$$\int_\Omega \Phi \cdot \left(\frac{\partial^2 p}{\partial x^2} + \frac{\partial^2 p}{\partial y^2} + \frac{\partial^2 p}{\partial z^2} \right) dxdydz$$

$$= \int_{\partial\Omega} \Phi \cdot \frac{\partial p}{\partial n} ds - \int_\Omega \left(\frac{\partial \Phi}{\partial x} \cdot \frac{\partial p}{\partial x} + \frac{\partial \Phi}{\partial y} \cdot \frac{\partial p}{\partial y} + \frac{\partial \Phi}{\partial z} \cdot \frac{\partial p}{\partial z} \right) dxdydz \tag{3}$$

where s is the area of the boundary and $\partial p/\partial n$ is the differentiation of the sound pressure to outward normal direction of the boundary $\partial\Omega$ in Fig. 1. In this case three boundary conditions for the sound field in a room can be considered as:

$$\frac{\partial p}{\partial n} = 0 \tag{4}$$

$$\frac{\partial p}{\partial n} = -j\rho\omega \frac{p}{Z_n} \tag{5}$$

$$\frac{\partial p}{\partial n} = -j\rho\omega v \tag{6}$$

where $j = \sqrt{-1}$

ρ = air density (kg/m³)

Z_n = normal sound impedance(kg/m² sec)

v = vibration velocity in normal direction(m/sec)

Substituting Eqs. (4), (5) and (6) into Eqs. (3), one has the following integration equation:

$$\int_\Omega \left[\left(\frac{\partial \Phi}{\partial x} \cdot \frac{\partial p}{\partial y} + \frac{\partial \Phi}{\partial y} \cdot \frac{\partial p}{\partial y} + \frac{\partial \Phi}{\partial z} \cdot \frac{\partial p}{\partial z} \right) - \Phi \cdot \frac{\omega^2}{c_0^2} p \right] dxdydz$$

$$+ j\rho\omega \int_{\partial\Omega_1} \frac{1}{Z_n} \Phi \cdot p \, ds = j\rho\omega \int_{\partial\Omega_2} \Phi \cdot v \, ds \tag{7}$$

As shown in Fig.2, the sound pressure p for an arbitrary point in an element can be approximated as:

$$p = \{\psi_i\}^T \{p_i\}^e \tag{8}$$

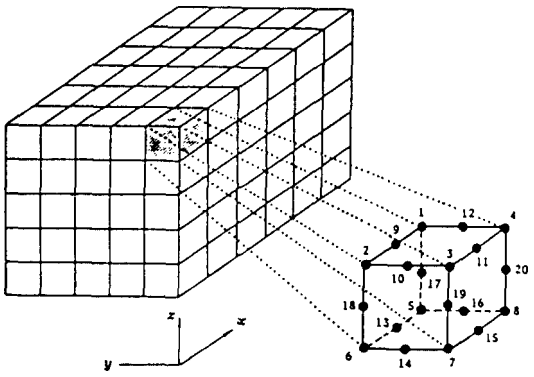

Fig. 2. Finite element discretization by 20 node iso parametric element.

where N_e is the number of nodes in each element, $\{\psi_i\}$ are shape functions in an element coordinate, $\{p_i\}$ is the sound pressure at a node, the superscript T is the transpose of a vector and the superscript e means a value for an element.

Assuming that weighting function Φ equals to shape function ψ, Eq. (8) yields from Eq. (7)

$$\int_{\Omega e}\left[\left(-\frac{\partial\{\psi_i\}}{\partial x}\cdot\frac{\partial\{\psi_j\}^T}{\partial x}+\frac{\partial\{\psi_i\}}{\partial y}\cdot\frac{\partial\{\psi_j\}^T}{\partial y}+\frac{\partial\{\psi_i\}}{\partial z}\cdot\frac{\partial\{\psi_j\}^T}{\partial z}\right)-\frac{\omega^2}{c_0^2}\{\psi_i\}\{\psi_j\}^T\right]\cdot\{p_i\}\,dxdydz+j\rho\omega\int_{\Gamma\Omega e}\frac{1}{Z_n}\{\psi_i\}\{\psi_j\}^T\{p_i\}\,ds=j\rho\omega\int_{\Gamma\Omega e}v\cdot\{\psi_i\}\,ds \tag{9}$$

$i, j = 1, 2, 3, \ldots N$

By integrating each term in Eq. (9) for an element and summing the results of all elemnts, N dimensional complex coupled first order equations are obtained in terms of the sound pressure at each node as follows :

$$([K]-\omega^2[M]+j\rho\omega[G])\begin{Bmatrix}p_1\\ \vdots\\ p_N\end{Bmatrix}=\{F\} \tag{10}$$

2.2 Finite Element Method for Sound Intensity

The complex sound pressures at all nodes in a sound field from Eq. (10) will be used to obtain a complex sound intensity. Denoting by p the complex sound pressure for a point s, and by v_x, v_y and v_z and v_{xs}, the components in x-, y- and z directions of a particle velocity, respectively, the sound pressures p_i at a node and shape functions ψ_i in an element are used to yield the following equations :

$$p_s=\sum_{i=1}^{N_e}p_i\cdot\psi_i \tag{11}$$

$$\left.\begin{aligned}v_x&=-\frac{1}{j\rho\omega}\cdot\frac{\partial p_s}{\partial x}\\ v_y&=-\frac{1}{j\rho\omega}\cdot\frac{\partial p_s}{\partial y}\\ v_z&=-\frac{1}{j\rho\omega}\cdot\frac{\partial p_s}{\partial z}\end{aligned}\right\} \tag{12}$$

where $\cdot$ means the known value.

Based on Eqs. (11) and (12), the net sound intensities, I_x, I_y and I_z of a point s in x-, y-, and z- directions, respectively, are described as follows :

$$\left.\begin{aligned}I_x&=\frac{1}{2}\,p\cdot v_x^*\\ I_y&=\frac{1}{2}\,p\cdot v_y^*\\ I_z&=\frac{1}{2}\,p\cdot v_z^*\end{aligned}\right\} \tag{13}$$

where $*$ is the complex conjugate.

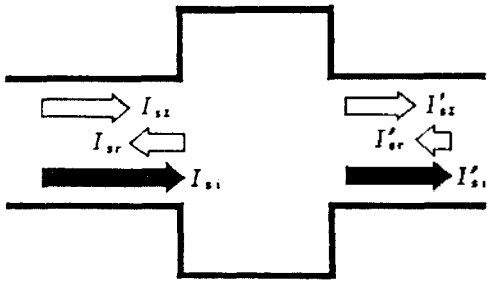

Fig. 3. Description of the sound intensities, I_{sx}, I_{sr} and I_{si}

2.3 Sound Transmission Loss in a Sound Attenuation Chamber

In order to obtain the sound transmission loss in a sound attenuation chamber (the level difference between input and output powers), the net sound intensity from Eq. (13) can be separated into the progressive and reflected sound intensities. The separation method will be explained in the following.

With one-dimensional sound field condition of the inlet and outlet ducts in x-direction as shown in Fig.3, the net sound intensity I_{sx} for an arbitrary point s in a duct has the following relations with the incident intensity I_{si} and the reflected intensity I_{sr} :

$$I_{sx} = I_{si} + I_{sr} = (1 - |\gamma|^2) \cdot I_{si} \tag{14}$$

where γ is the reflection coefficient of complex sound pressure. It is noted that the separation of progressive and reflected intensities is possible when the I_{sx} and γ are known. For the finite element method mentioned above, the γ can be obtained in terms of the complex sound pressure p_s and a particle velocity v_{sx} based on Eq. (13) as follows :

$$\gamma = \frac{\dfrac{p_s}{v_{sx}} - \rho c}{\dfrac{p_s}{v_{sx}} + \rho c} \tag{15}$$

where ρc is the specific acoustic impedance.

Finally, the transmission loss can be expressed in terms of incident sound power W_i and transmitted sound power W_t as :

$$TL = -10 \cdot \log_{10} \frac{W_t}{W_i} \tag{16}$$

III. Measurement Principle

The principle of the cross spectrum intensity method will be discussed. For the measurement of impedance in a general sound field, Lahti[5] suggested the following relations :

$$Z = \frac{j\omega\rho\Delta r}{2} \cdot \frac{G_{11} + G_{22} + 2 \cdot \mathrm{Re}\{G_{12}\}}{G_{11} - G_{22} - j2 \cdot \mathrm{Im}\{G_{12}\}} \tag{17}$$

where G_{11} and G_{22} are the auto-spectrum density functions of the sound pressure at two points spaced by the distance Δr, respectively, and G_{12} is the cross spectrum density function between them.

Based on the principle of the cross-spectrum intensity method[6], the net sound intensity I_{sx} is expressed as :

$$I_{sx} = -\frac{\mathrm{Im}\{G_{12}\}}{\omega\rho\Delta r} \tag{18}$$

i. e. the progressive and reflected sound intensities will be obtaied similarly as in the numerical analysis mentioned above if the autospectrum and cross-spectrum are measured using the two microphone method. Consequently, the sound transmission loss can be obtained.

IV. Applications

4.1 FEM Analysis

For the models in Fig. 4, which describes a simple expansion and multi-plenum type sound attenuation chambers, numerical analyses are carried out to estimate the transmission loss. As the boundary conditions, a vibrating plane of constant velocity was assumed at the end of the inlet duct

and ρc is the termination impedance at the end the outilet duct. The sound field for the chambers and ducts was analyzed by the three dimensional FEM model. In the process a 20 node hexahedral finite element is used, and the size of an element is chosen to be less than 1/4 of the maximun wave length in the numerical analysis. The half of the sound field is considered because of the symmetry of the upper and lower parts. The results were obtained from 28 Hz to 340 Hz (c_0=343 m/sec) by every 1 Hz. It is noted that one-dimensional sound field condition is satisfied at 340 Hz at the inlet and outlet ducts in chamber.

The inside conditions of two models are described as follows.

MODEL-1 (an expansion-type chamber)

TWPE-I : without absorption

TYPE-II : with acoustic impedance

TYPE-III : with a partition wall (without absorption)

MODEL 2 (a multi-plenum chamber)

TYPE-A : without a partition wall (without absorption)

TYPE-B : with a partition wall of 0.75m length

TYPE-C : with a partition wall of 1m length

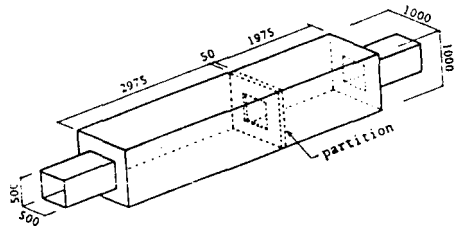

(a) Expansion chamber

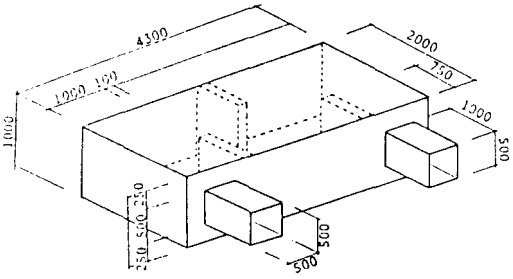

(b) Multi-plenum chamber

Fig. 4. FEM analysis experimental model.

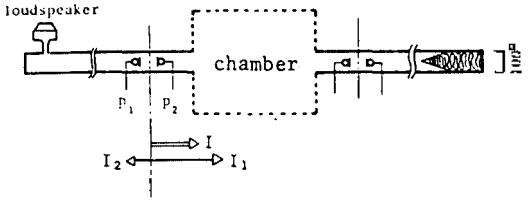

Fig. 5. A 1/5th scale model experiment system

4.2 Scale Model Experiments

In order to compare with the numerical analyses, the chambers with the inlet and outlet ducts described above were simulated by 1/5 scale models with a vinyl chloride plate of 10mm thickness. As shown in Fig. 5, a square duct of 1m length (cross-sectional area : 100㎠, cut-off frequency : 1700Hz) are connected to each end of the sound attenuaton chamber. For the sound source, a loudspeaker (horn driving unit) was attached to the end of the inlet duct and broad band noise was radiated, while the end of the outlet duct was terminated with the glass fiber board to make it absorptive. In order to make the measurement reliable, the intensity measurements were performed at six points in each measurement cross-section and the spatial-mean values of G_{11}, G_{22} and G_{12} were obtained. An intensity probe consisited of two 1/4 inch condenser microphones (B&K 4718) with 12mm gap was used and their output signals were analyzed by using FFT processor (B&K 2032).

4.3 Results and Discussions

For the expansion chamber TYPE I (without absorption) Fig. 6 shows the comparison of the transmission loss by numerical analysis with experimental result. Although the peak and dip frequencies have a slight discrepancies, both

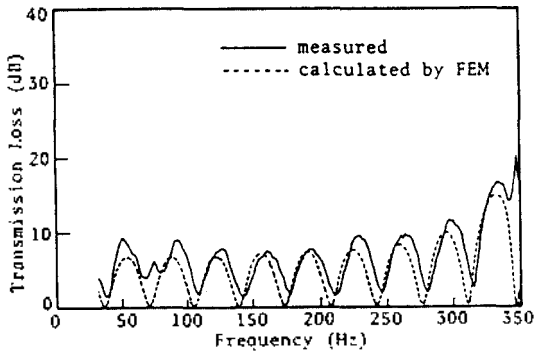

Fig. 6. The transmission loss of the expansion TYPE I chamber(without absorption)

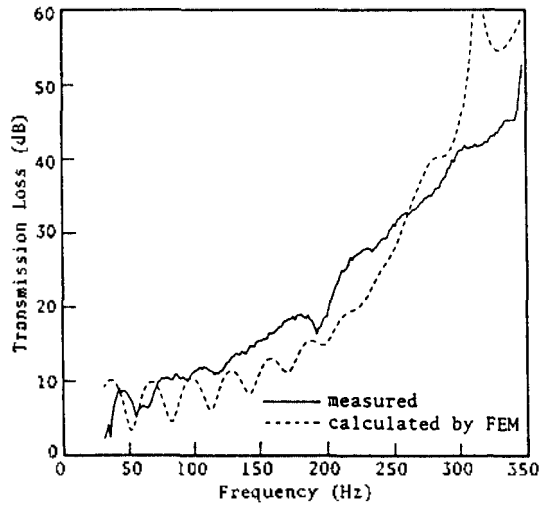

Fig. 7. The transmission loss of the expansion TYPE-II chamber(with absorption)

results are fairly in good agreement up to the cut-off frequency of the inlet and outlet ducts (340 Hz in real frequecny). For the chamber TYPE-I, the theoretical solution can be obtained from Davis' Equation [7]. As a result, it has been found that the result of FEM is precisely agreed with the mathematical solution up to the cut off frequency of the expansion duct(170 Hz in real frequency).

Fig. 7 shows the result for the case that a partition wall of a chamber (TYPE-II) was made absorptive. For the boundary condition of FEM, the normal impedance of the glass fiber board measured by the acoustic tube method was applied. As a result, it can be seen that both results are in partial agreement on the whole :

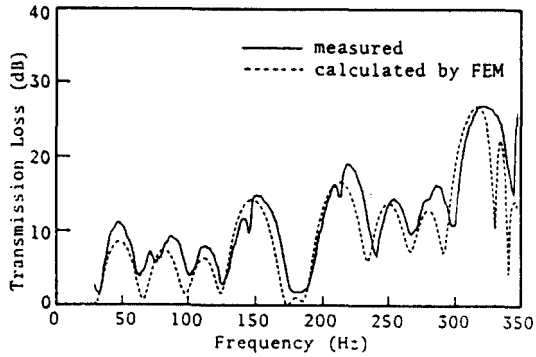

Fig. 8. The transmission loss of the expansion TYPE-III chamber(without absorption)

In Fig. 8 the characteristics of the transmission loss for TYPE III, in which a partition wall added in a MODEL 1 chamber, were shown. Depending on the frequencies, the transmission loss have slightly different values ; however, the both results indicate consistent phenomena caused by a partition wall. In Figs. 6 and 8 the transmission loss is described for the cases that a partition wall located in a chamer.

The results of the numerical analysis for multi-plenum chamber of MODEL-2 are shown in Fig. 9. In the process the sound is assumed to be absorbent (Impedance Z 80000kg/m² sec) inside a sound attenuation chamber in consideration of the sound absorbent condition at the inner face of a scale model. Although both numerical and experimental results have some discrepancies in the range of high frequencies around 200 Hz, two results are well agreed for the estimation of the sound transmission loss, depending on the existence and the length of a partition wall. For a reference, Fig. 10 shows the result of transmission loss in combination with 1/3 octave band for TYPE C of MODEL 2.

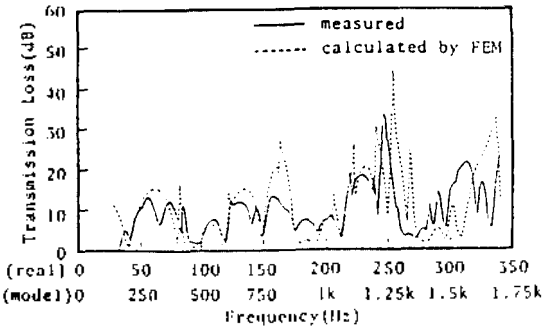

(a) Without partition

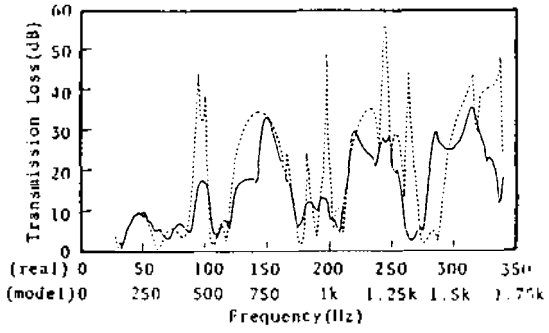

(b) Partition length 0.75m

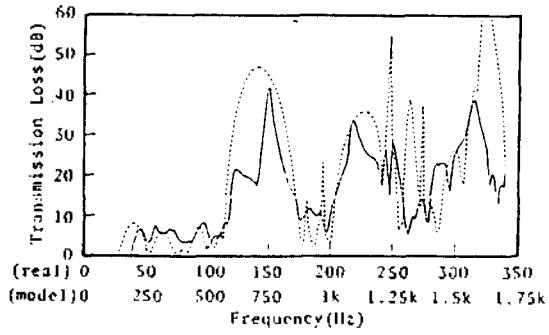

(c) Partiton length 1m

Fig. 9. The transmission loss of the multi plenum chamber(without absorption)

V. Conclusion

A new FEM algorithm was proposed to estimate the sound transmission loss in the sound attenuation chamber by separation the net sound intensity in a steady state sound field obtained from FEM into the progressive and reflected

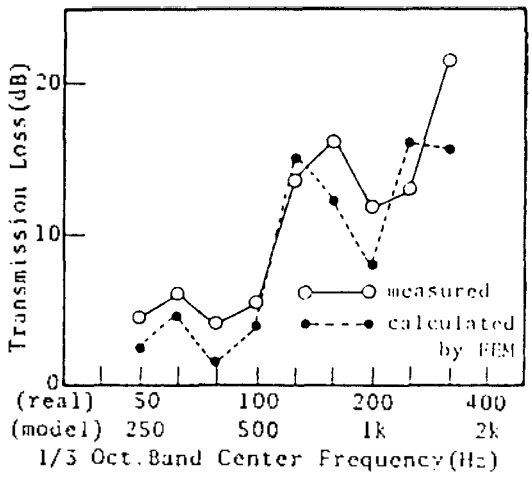

Fig. 10. The transmission loss of TYPE C chamber in combination with 1/3 octave band

intensities. A cross-spectrum method was also discussed as an estimation method for the transmission loss in a real measurement system. God agreement between the nemurical analyses and the experiments indicates that the proposed approach for the sound transimssion loss is very effective.

REFERENCES

1. Y.Kagawa, T.Yamabuchi and A.Mori, "Finite element simulation of an axisymmetric acoustic transmission system with a sound absorbing wall," J. Sound and Vib., Vol.53(3), pp.357-374(1977).
2. J.F.Unruh and W.Eversman, "The utility of the Garerkin method for the acoustic transmission in an attenuating duct," J.Sound and Vib., Vol.23(2), pp.187-197(1972).
3. R.J.Astley and W.Eversman, "A finite element formulation of the eigenvalue problem : an improved formulation using Hemitian elements and flow condensation," J. Sound and Vib., Vol.69(1), pp.13-25 (1980).
4. S.J.Choi and H.Tachibana, "Estimation of impulse response in a room by the finite element method," J.Acoust. Soc. of Jpn(J), Vol.49(5), pp.328-333 (1993).
5. T.Lathi, 2nd International Congress on acoustics Intensity, pp.519-526(1985).

6. F.J.Fahy, "SOUND INTENSITY," ELSEVIER APPLIED SCIENCE(1989).
7. D.D.Davis, Jr., "Acoustical Filters and Mufflers," in C.M.Harris, Handbook of Noise Control, chap.21, McGraw Hill(1957).

▲Seok Joo Choi

Seok Joo Choi Born on January 11 1957 in Jeonbuk do, Korea. Graduated from Jeonbuk National University in 1980, and received Engineering Doctor from Tokyo University in 1990. Senior researcher of Institute of Technology, Samsung Engineering and Construction Co. Ltd.

▲Hideki Tachibana

Hideki Tachibana Born on August 23 1943 in Tokyo, Japan. Graduated from Tokyo University in 1967, and received Engineering Doctor from Tokyo University in 1973. Professor of Institute of Industrial Science, Tokyo University. Head of the Applied Acoustic Engineering Laboratory.